Ryszard Kwiatkowski*[1],
Andrzej Włochowicz[1],
J. Kozakiewicz[2],
J. Przybylski[2]

[1]University of Bielsko-Biała,
43-309, Willowa 2, Bielsko-Biała, Poland,
*rkwiatkowski@ath.bielsko.pl
[2]Industrial Chemistry Research Institute,
01-793, Rydygiera 8, Warszawa, Poland

WAXS and SAXS study of (m)TMXDI-PDMS siloxane-urethaneureas

Abstract

The results of WAXS and SAXS investigations of moisture-cured (m) TMXDI-SODI siloxane-urethaneureas are presented. The SODI siloxane soft segment of the urethanes investigated included 20 dimethylsiloxane (DMS) units and the TMXDI di-isocyanate concentration, determined by the NCO/OH ratio was equal to 1.5/1, 2.0/1, 2.5/1 3.5/1 and 4.5/1. Consequently, the mean length of siloxane-urethane prepolymers of these urethanes decreased from ca. 4 to ca. 1 [-TMXDI-SODI-] unit, as is determined from GPC measurements, and the mean length of TMXDI hard segments in moisture-cured TMXDI-SODI films gradually increased, as is indicated by ATR-FTIR measurements of these films. Both WAXS and SAXS measurements reveal a distinct domain separation between TMXDI hard segments and siloxane-rich soft segments in TMXDI-SODI films. The combined WAXS and DSC measurements clearly show that longer TMXDI hard segments are mutually arranged. A resolution of WAXS patterns of TMXDI-SODI siloxane-urethaneureas into diffraction peaks and diffuse maxima is performed. Agreement is shown between the Bragg spacing attributed to the most intense WAXS diffraction peak and the fibre identity period of a molecular model of an extended (-TMXDI-UR-) chain (UR-urea bond). Only a single SAXS diffraction maximum is found to appear in SAXS patterns of TMXDI-SODI films, and a gradual increase in an identity period of the superstructure of TMXDI-SODI films is found when the NCO/OH ratio increases. Moreover, a gradual increase in the normalised invariant of films investigated is found when the NCO/OH ratio increases. This effect is mostly attributed to a gradual increase in an electron density contrast between TMXDI hard and siloxane rich soft domains. A lamellar face superstructure is postulated for each TMXDI-SODI urethane. The influence of the concentration of the TMXDI units on the long period and on the thickness of both hard and soft layers in lamellar stacks of TMXDI-SODI urethanes is determined.

Key words: *urethanes, siloxane-urethaneureas, WAXS, SAXS, morphology.*

1. Introduction

It is well known that the particular chemical structure of segmented urethanes is reflected in both their supermolecular structure and fundamental properties [1,2]. Due to the distinct chemical incompatibility of soft and hard segments, a phase separation occurs in segmented urethanes, and as a consequence a specific domain structure is formed [3-10]. Hard domains, which act as physical links distributed in a soft matrix, determine the physical properties of these polymers. Two broad classes of urethanes which are commonly used are based on ether or ester oligomer diols as a soft segment of segmented urethane chains. The third class of urethanes are siloxane urethanes, which play a very important role in specific technical and medical applications due to the unusual properties of the $(DMS)_n$ dimethylsiloxane chain [11-18]. These urethanes link the excellent mechanical properties of urethanes with biocompatibility, water-repellence, temperature resistance and the gas permeability of silicones in one superb material.

Recently, extensive studies on such materials at the Industrial Chemistry Research Institute in Warszawa have led to the development of a novel way of producing moisture-cured siloxane-urethaneureas (MCPSUUR) intended first of all for coating applications [19,20]. These urethanes are prepared from a di-isocyanate and siloxane oligomer diols, hereafter referred to as SODI and SODII, which are terminated by aliphatic-ether (SODI) or aliphatic (SODII) chain extenders, capped by OH hydroxyl groups. The synthesis is based on a two-step process. During the first step, siloxane-urethane prepolymers (whose molecules consist of SOD and diisocyanate units linked to SOD by urethane bonds) are synthesised. The second step is a moisture-curing process (MC) which proceeds in a very complex way. During the curing, both the siloxane-urethane prepolymers and free diisocyanate units (i.e. the diisocyanate units which have not reacted due to their excess) simultaneously link among themselves by urea bonds. Both the chemical structure of substrates and an example scheme of a chain of siloxane-urethaneureas produced from the (m)TMXDI diisocyanate and the SODI siloxane oligomer diol as the soft segment are presented in Fig. 1.

As expected, the length of di-isocyanate sequences in TMXDI hard segments should increase with the increase in the concentration of the free di-isocyanate units in a prepolymer, and a phase separation should occur in the cured TMXDI-SODI films due to the distinct chemical incompatibility of siloxane soft segments and TMXDI hard segments [21,22]. Hence, the dimensions of di-isocyanate hard domains should also increase. The aim of this work was to reveal the phase separation and the domain structure of these novel TMXDI-SODI siloxane-urethaneureas, and to determine the dependence of interdomain dimensions on the concentration of TMXDI di-isocyanate units. WAXS and SAXS methods have been employed for this goal. X-ray scattering measurements were carried out for a series of TMXDI-SODI siloxane-urethaneureas for which the length of SODI siloxane soft segments was constant and the concentration of TMXDI units, determined by the NCO/OH ratio, was changed from 1.5/1 to 4.5/1.

2. Experimental

2.1. Raw materials, synthesis and characteristics of the investigated siloxane-urethaneureas

The raw materials used for the synthesis of the urethanes investigated included the tetramethylxylilenediisocynate (TMXDI) produced by the American Cyanamid Co., and the KF-6001 siloxane oligomer diol (the SODI structure in Fig. 1 which

consists of 20 DMS units) produced by the Shin-Etsu Co.

The synthesis of the siloxane-urethane prepolymers and the moisture curing of these prepolymers to TMXDI-SODI siloxane-urethaneureas were carried out at the Industrial Chemistry Research Institute in Warszawa. Liquid viscous siloxane-urethane prepolymers were synthesised following a standard procedure for synthesising urethane prepolymers [23]. The concentration of TMXDI units was controlled in accordance with the following values of NCO / OH ratio: 1.5 / 1; 2.0 / 1; 2.5 / 1; 3.5 / 1 and 4.5 / 1. For each prepolymer, both the viscosity (η) and the molecular masses M_n and M_w were measured to eslish the changes in the mean length of siloxane-urethane prepolymers when the di-isocyanate concentration increases (the η viscosity was determined by the Brookfield method, and the M_n and M_w molecular masses were determined by the GPC method using a Shimadzu CR4A Chrompac instrument calibrated for polystyrene reference samples). The ratio of the M_n mass to the molecular mass of the [-TMXDI-SODI-] constitutional unit of siloxane-urethane prepolymers was used as a quantitative measure of the l_M mean length of these prepolymers [24]. Moreover, the content of reactive isocyanate groups in prepolymers was determined by the dibutylamine back-titration method (that is, the %NCO content per the unit mass of a prepolymer). In order to prepare a given siloxane-urethaneurea sample, a thick layer (of ca. d_f =0.5-1 mm) (Tab.1) of a given liquid viscous prepolymer was coated onto a PTFE plate; then the curing of the film was performed in a special chamber at a constant temperature (25°C) and humidity (50%). The symbols and characteristics of both siloxane-urethane prepolymers and siloxane-urethaneurea films prepared are given in Tab.1.

To control whether isocyanate groups have reacted during the curing process, the ATR-FTIR method was used to monitor both the C=O urethane band and especially the C=O urea band [25]. The ATR-FTIR measurements were made on the MAGNA-860 spectrometer. The ATR spectra of TMXDI-SODI films investigated are superimposed in Fig. 2. A distinct gradual increase in the intensity of the C=O urea band is clearly visible (the ATR spectra were normalised to an intensity of the Si-Me band).

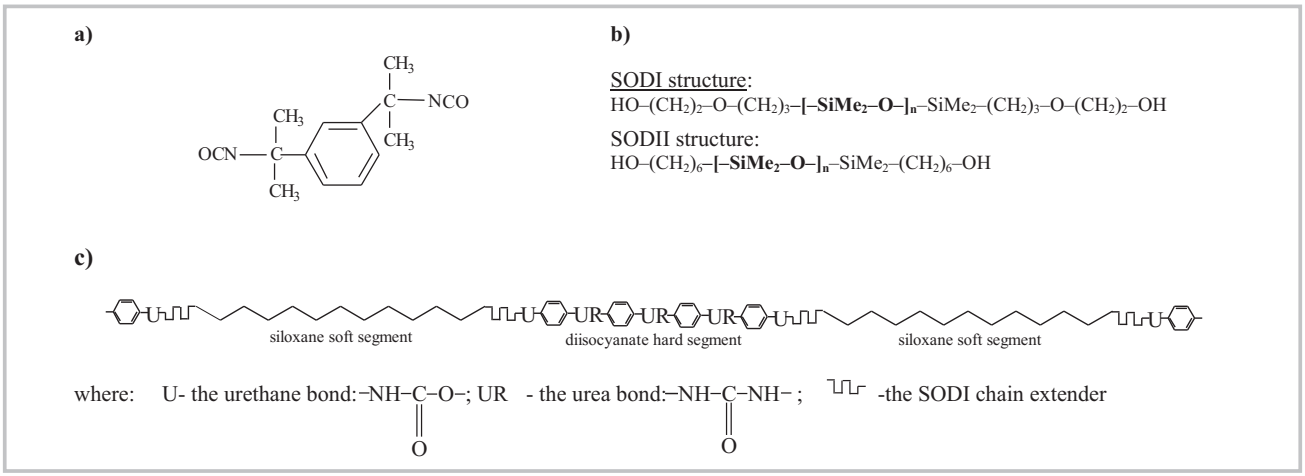

Figure 1. *Scheme of unit structures and an example chain structure of (m)TMXDI-SODI siloxane-urethaneureas: a) the chemical structure of the (m)* ***TMXDI*** *diisocyanate, b) the chemical structure of the SODI and the SODII siloxane soft segments, c) a scheme of a segmented TMXDI-SODI siloxane -urethaneurea chain.*

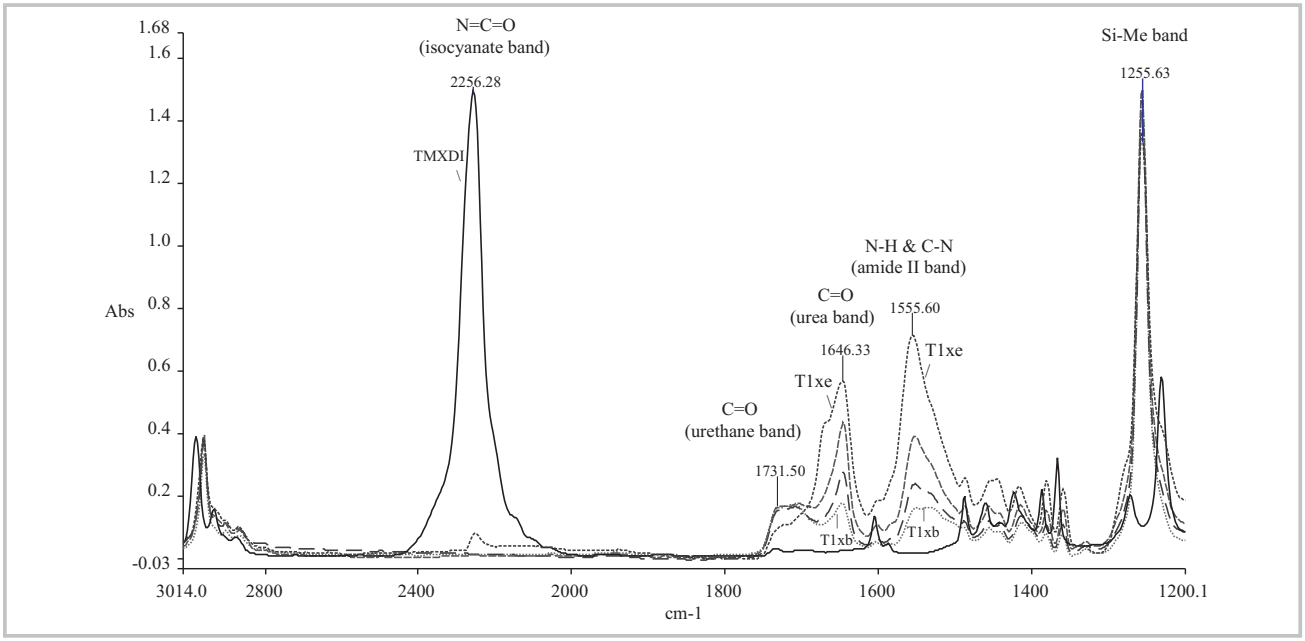

Figure. 2. *The comparison of ATR spectra of siloxane-ureaurethane films and the FTIR spectrum of the TMXDI di-isocyanate.*

Table 1. The characteristics of the TMXDI-SODI siloxane-urethane prepolymers and siloxane-urethaneurea films.

symbol	NCO/OH	%NCO	M_n	M_w	M_w/M_n	η [cP]	I_M	d_f [mm]	T
T1xa	1.5/1	1.85	7830	19120	2.5	2190	3.8	0.3	0.439
T1xb	2.0/1	3.64	5010	10900	2.1	870	2.4	0.65	0.275
T1xc	2.5/1	5.43	3990	8050	2.0	412	1.9	0.92	0.172
T1xd	3.5/1	8.05	3530	6750	1.9	215	1.7	0.57	0.367
T1xe	4.5/1	10.34	2164	6174	2.8	177	1.0	1.11	0.232

2.2. X-ray measurements and data processing

For both SAXS and WAXS measurements, a Cu target X-ray tube was used as a radiation source (λ = 1.542 Å), operated at U= 40 kV and I= 30 mA.

The SAXS measurements were made on a Kratky compact camera, equipped with the HECUS-MBRAUN optical system. The scattered radiation was detected by an OED-51 linear position sensitive counter. The resolution of these SAXS measurements was 600 Å (as determined by the Bragg spacing corresponding to a first measurement point). The moving slit method [26] was employed to determine the T transmittance factor (Tab.1) for each film investigated. The experimental SAXS patterns were smoothed, and then the background was subtracted using the Vonk approximation [27] of a small-angle scattering background. After being corrected in this way, the SAXS patterns were desmeared by using the direct method of the desmearing procedure [28] implemented on HECUS-MBRAUN software; then the correlation functions were calculated by using the OTOKO computer program elaborated by Dr Koch [29].

The WAXS measurements were carried out on a URD-6 Seifert diffractometer, equipped with a graphite monochromator. The step scanning mode was employed in the range of the 2θ scattering angle from 1° to 60° with the step of 0.1°. The WAXS patterns of the investigated films were resolved into Gaussian shape diffraction maxima by using the Levenber-Marquardt non-linear fitting procedure implemented on ORIGIN 6.1 software.

3. Results and discussion

3.1. WAXS measurements

The WAXS diffraction patterns of TMXDI-SODI films are shown in Fig. 3. In general, the WAXS curve for each TMXDI-SODI siloxane-urethaneurea consists of an intense and relatively narrow diffraction maximum centred at ca. 12° and a broad diffraction maximum centred at ca. 18°. When both the number and the mean length of hard segments increase due to the increase of TMXDI units concentration, i.e. when the NCO/OH ratio is greater then 2.5/1, a clearly visible small diffraction peak starts to appear as a top (centred at ca. 20°) of the broad diffraction maximum, and additionally a complex diffusion scattering is observed in the range from 30° to 50° of the 2θ scattering angles. Moreover, one may observe that the intensity of the diffraction maximum at 12° and of the top at 20° increases with the increase of the NCO/OH ratio. These findings strongly indicate that the supermolecular structure of these siloxane-urethaneureas consists of TMXDI hard domains distributed in a siloxane-rich soft matrix, and that TMXDI hard segments form a more or less ordered structure depending on a hard segment content, and consequently most probably depending on the mean length of TMXDI sequences.

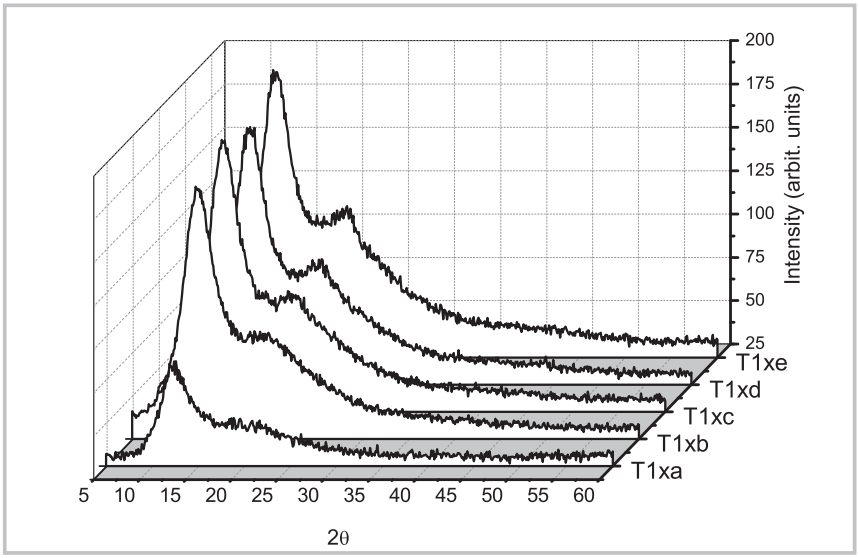

Figure 3. WAXS diffraction patterns of TMXDI-SODI siloxane-urethaneurea films.

The suppositions as above are supported by the results of the combined DSC and WAXS measurements. For instance, four endotherms were detected in the range from 60°C to 180°C for the T1xd film, as shown in Fig. 4.a. In Fig. 4.b the WAXS patterns of this film are superimposed. They have been measured at room temperature after heating and 1h annealing of the film at temperatures close to the end of those endotherms (i.e. at: 90, 133, 152 and 171°C). As seen in Fig. 4.b, a decrease in the intensity of diffraction peaks is observed after thermal treatments at 133 and 152°C. After the last annealing at 171°C, numerous very sharp diffraction peaks appear in the WAXS curve, which indicate both the decomposition of this siloxane-urethaneurea and the crystallisation of the product of this decomposition. It is well known that for MDI/BDO urethanes multiple high-temperature endotherms occur in the temperature range from ca. 50 to ca. 250°C [30-36]. These are assigned to thermal transitions of hard domains: in other words, the first endotherm is ascribed to a short-range order of unknown nature, or to some relaxation effects in the hard segment phase; the second is attributed to a hard segment long-range order of unspecified nature, or to the onset of the phase mixing; and the third (usually observed above 200°C) is attributed to the melting of hard segment micro-crystalline regions. (The details of the DSC measurements of the urethanes investigated here will be presented in a separate paper). Thus, the thermally induced behaviour of the intense diffraction maximum at ca. 12° and of the diffraction peak at ca. 20° clearly indicate both a short-range and a long-range mutual arrangement (i.e. probably a paracrystalline long-range arrangement) of the TMXDI hard segments which form hard domains in TMXDI-SODI siloxane-urethaneureas. Consequently, one may postulate that

the intense diffraction maximum at ca. 12° is complex, i.e. that this maximum is composed of two diffraction peaks attributed respectively to a less and more ordered structure of TMXDI hard domains. Example resolutions of WAXS diffraction patterns of the T1xd and the T1xb film into diffraction peaks and the diffuse diffraction maxima obtained under this assumption are shown in Fig. 5.

As seen in Fig. 5, the complex diffusion scattering in the range of 2θ from 30° to 50° is resolved into two Gaussian shape diffuse maxima. One may suppose that this is a consequence of a distinct difference between interatomic distances in the (-Si-O-Si-) siloxane chains and interatomic distances in other parts of a siloxane-urethaneurea chain. Finally, as a result of such a resolution of WAXS patterns of TMXDI-SODI films, one may conclude that those three relatively broad diffuse maxima, i.e. the maxima centred at ca. 2θ ≈ 18°, 30.0° and 40.0°, are attributed to X-ray scattering by amorphous siloxane rich soft phase and transition zones. The data of the 2θ angular position and the Bragg spacing (d = λ/2sin θ) of diffraction peaks, the angular position, and the Bragg spacing of amorphous diffraction maxima and values of the relative integral intensity (A%) of these peaks and maxima, determined by the resolution of WAXS pattern of each investigated film, are collected in Tab. 2.

First of all, the data collected in Tab.2 show that the integral intensity of components of the complex diffraction maximum centred at ca. 12° changes in the opposite way when the NCO/OH ratio increases. The intensity of the first component (the diffraction peak centred at 2θ ≈ 11.8°; d ≈ 7.50 [Å]) increases, and simultaneously the intensity of the second component (the diffraction peak centred at 2θ ≈ 12.0°; d ≈ 7.34 [Å]) decreases with the increase in the NCO/OH ratio. Moreover, the first peak is narrower in comparison to the second one, as seen in Fig. 5. Hence, one may attribute this first peak to X-ray scattering by a more ordered structure formed by longer TMXDI hard segments, and the second peak to X-ray scattering by a less ordered structure formed by shorter TMXDI hard segments. Besides, it should be noted that a gradual increase in the integral intensity of the small diffraction peak occurs with the increase in the NCO/OH ratio (the diffraction peak centred at 2θ≈ 19.7°; d ≈ 4.5 [Å]). In accordance with theoretical predictions, the Bragg spacing related to the first diffraction peak may be assigned to an identity period of an extended (-TMXDI-UR-) chain which is the equivalent of the TMXDI sequences. The projection of an optimised model of the chain, obtained by using the MM+ potential force field of molecular modelling and

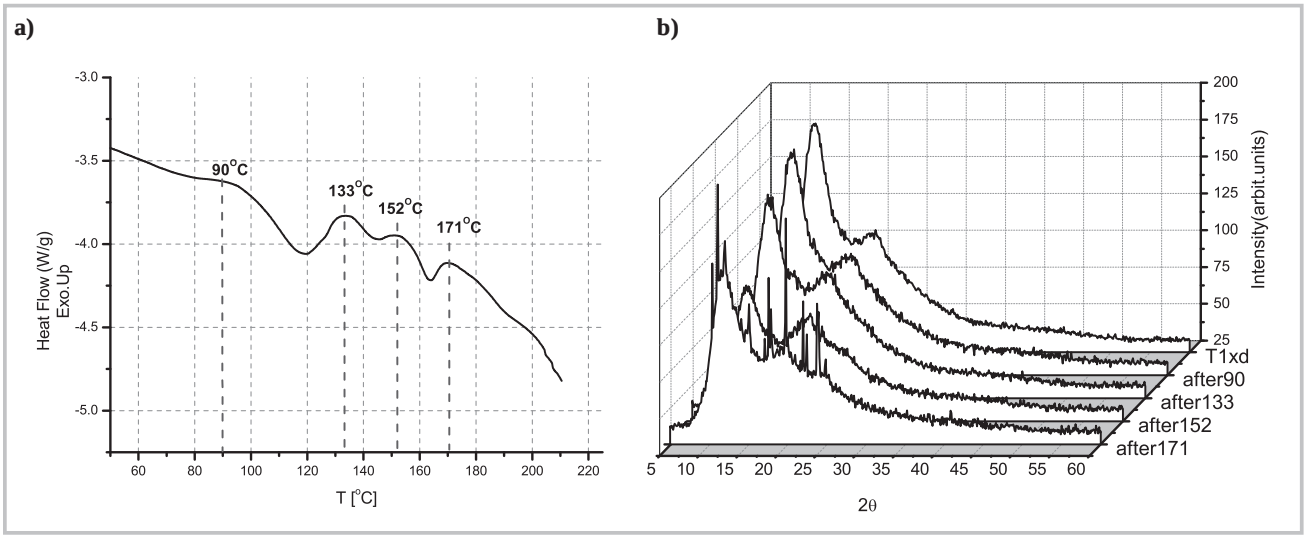

Figure 4. a) *The DSC thermograph of the T1xd sample,* ***b)*** *WAXS patterns of the annealed T1xd sample.*

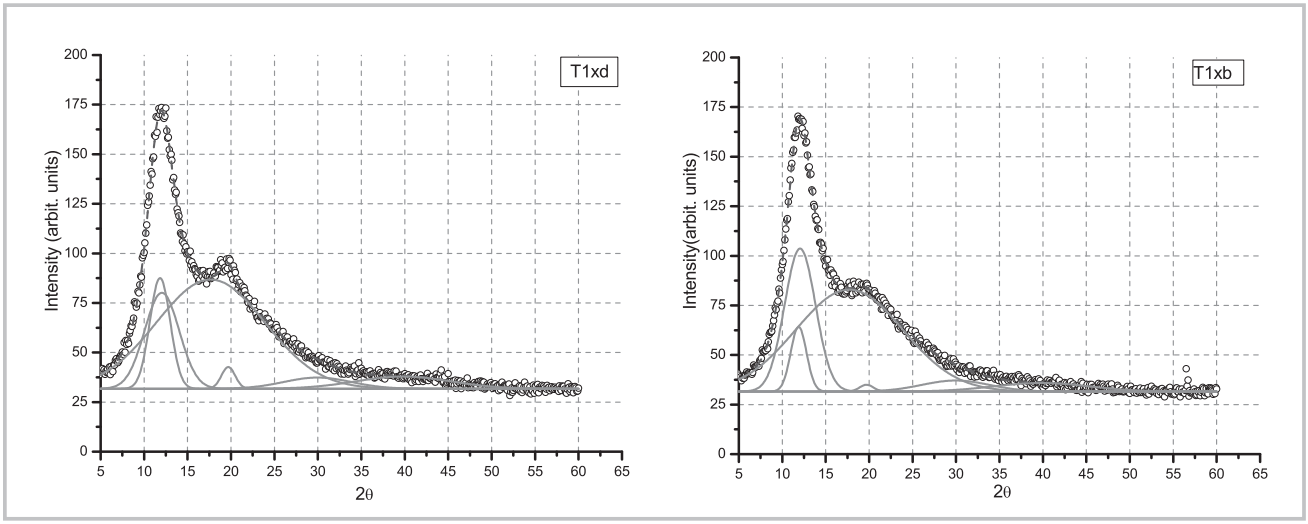

Figure 5. *An exemplary resolution of WAXS diffraction patterns of the T1xd sample (left side) and T1xb sample (right side).*
(····· the experimental curve; – – – the best fitted curve; —— Gaussian shape peaks and diffuse maxima).

the MNDO semi-empirical method, is shown in Fig. 6.

As depicted in Fig. 6, the [-TMXDI-UR-TMXDI-UR-TMXDI-] unit is the identity period of that extended chain conformation. Hence, the distance between the geometric centres of the phenyl rings which cap the unit is a measure of the fibre identity period of the (-TMXDI-UR-) chain. As was estimated from the model, the fibre identity period of the chain is equal to l_{fp} = 14.7 [Å]. The half of this value is very close to the Bragg spacing related to the $2\theta_1$ angular position of the first diffraction peak in the WAXS diffraction patterns of TMXDI-SODI siloxane-urethaneureas (d ≈ 7.50 [Å]; see Tab. 2 and Fig. 5). This agreement suggests the (002) Miller index should be attributed to this peak. Consequently, one may suppose that the small diffraction peak centred at ca. 19.70° (d ≈ 4.50 [Å]) reflects an interchain distance in TMXDI hard domains consisted of longer extended TMXDI hard segments. It is obvious that these segments can more readily be mutually arranged.

Table 2. *The data obtained from the resolution of WAXS patterns of TMXDI-SODI films.*

Sample		T1xa	T1xb	T1xc	T1xd	T1xe
NCO/OH		1.5/1	2.0/1	2.5/1	3.5/1	4.5/1
diffraction peaks	$2\theta_1$	11.99	11.88	11.81	11.83	11.80
	d [Å]	7.38	7.45	7.49	7.48	7.50
	A %	4.2	5.7	10.3	11.5	12.7
	$2\theta_2$	12.45	12.05	12.05	12.05	12.05
	d [Å]	7.11	7.34	7.34	7.34	7.34
	A %	25.9	24.5	20.2	16.9	14.9
	$2\theta_3$	-	19.69	19.69	19.69	19.69
	d [Å]	-	4.51	4.51	4.51	4.51
	A %	-	0.5	1.1	1.5	1.6
diffusion maxima	$2\theta_4$	19.38	17.71	17.73	17.65	17.81
	d [Å]	4.51	5.01	5.00	5.02	4.98
	A %	69.9	60.6	60.1	60.3	59.9
	$2\theta_5$	-	29.96	29.96	29.96	29.96
	d [Å]	-	2.98	2.98	2.98	2.98
	A %	-	4.1	3.3	3.8	4.5
	$2\theta_5$	-	39.85	39.85	39.85	39.85
	d [Å]	-	2.26	2.26	2.26	2.26
	A %	-	4.5	5.0	6.0	6.4

3.2. SAXS measurements

Fig. 7 shows the desmeared one-dimensional SAXS curves of siloxane-urethaneurea films under investigation which were normalised to arbitrary units, i.e. Iq^2 vs. q scattering functions normalised with respect to both the T transmittance factor and the d_f thickness of a sample [37] (where q is the magnitude of the scattering vector: $q=4\pi \sin\theta/\lambda$ [Å^{-1}]; 2θ is a scattering angle). As seen on the left side of this figure, a single distinct small-angle scattering maximum is observed for each siloxane-urethaneurea film. The angular position of these maxima depends on the TMXDI unit concentration, i.e. the greater the NCO / OH ratio, the closer to the zero of the q scale is the position of the scattering maximum. The normalised

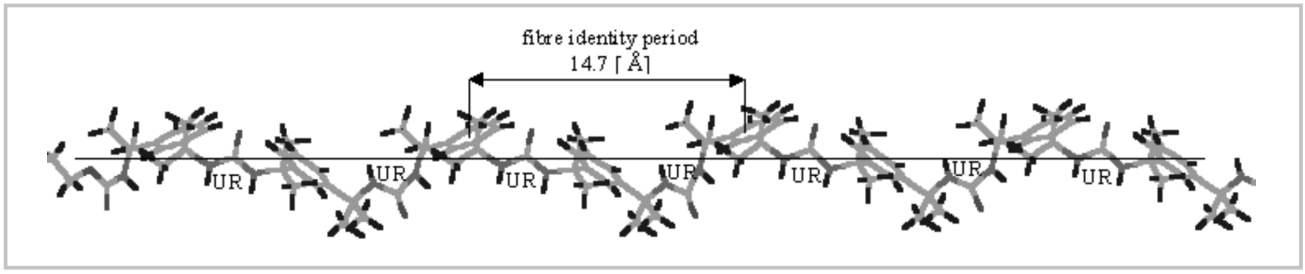

Figure 6. *The projection of an optimised model of (-TMXDI-UR-) chain as the equivalent of TMXDI sequences.*

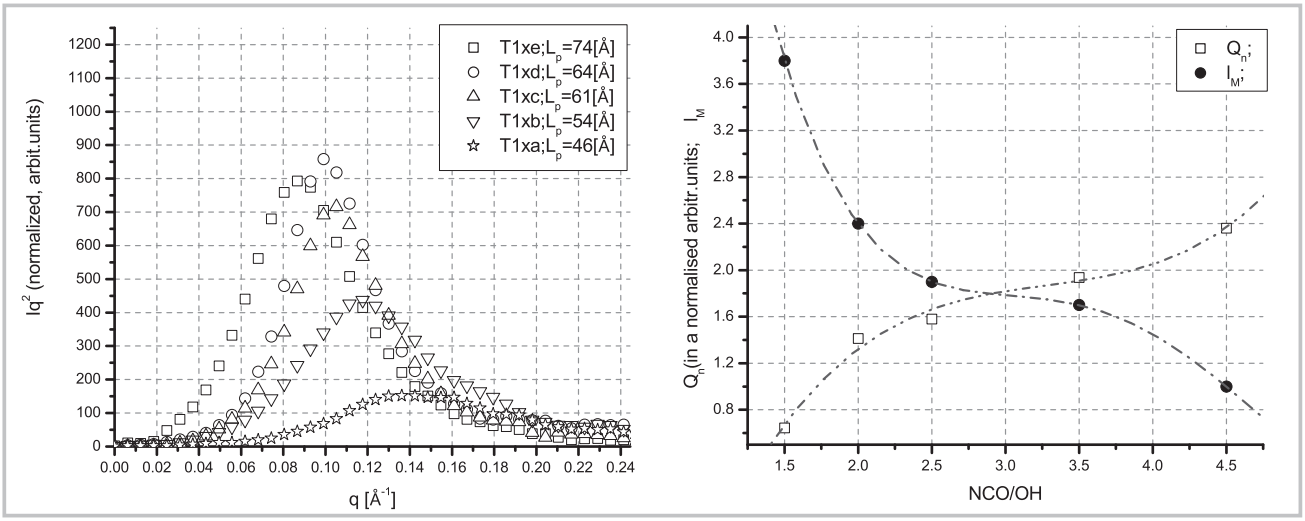

Figure 7. *Left: the comparison of desmeared Iq^2 SAXS curves of the investigated TMXDI-SODI films. (I - normalised to an intensity of arbitrary units; q - a scattering vector magnitude). Right: the comparison of the changes in the Q_n invariant of TMXDI-SODI films, normalised to arbitrary units, with the changes in the l_M mean length of siloxane-urethane prepolymers.*

integral intensity of these maxima increases with the increase in the NCO / OH ratio, and as a consequence the Q_n normalised invariant

$$Q_n = \int_0^\infty Iq^2 dq \qquad (1)$$

[37,38] increases with the increase in NCO / OH ratio, as shown on the right side of Fig. 7. It should be noticed that the changes in the Q_n invariant coincide well with changes in the l_M mean length of siloxane-urethane prepolymers as is shown on the right side of Fig. 7.

Considering both the results of the WAXS measurements presented earlier and the results of the SAXS measurements, one may postulate that the so-called supermolecular structure of the investigated siloxane-urethaneurea films has a lamellar structure face, and that the lamellar structure of these films consists of alternately stacked TMXDI hard domains and siloxane-rich soft domains. Upon this assumption, the L_{pw} weight average long period [37] of the lamellar structure for each film was determined directly from the position of the small-angle scattering maxima of the SAXS curves presented in Fig. 7, in accordance with the relationship $L_{pw} = 2\pi/q_m$ (where q_m is the position of a given SAXS maximum). In accordance with the data obtained, the long period of the lamellar structure of siloxane-urethaneurea films gradually increases with the increase in the TMXDI unit concentration (the values of the L_{pw} long period for each film are given in Fig. 7 and also collected in Tab. 3). The details of the lamellar structure of siloxane-urethaneurea films (the data are collected in Tab. 3) have been determined from the Vonk normalised γ(x) one-dimensional correlation function [27,37], calculated for each scattering function presented in Fig. 7 following equation (2) [27]:

$$\gamma(x) = \frac{\int_0^\infty I(q)\, q^2 \cos qx \, dq}{\int_0^\infty I(q)\, q^2 \, dq} \qquad (2)$$

These correlation functions are shown on the left side in Fig. 8. On the right side of this figure, the graphic analysis of the γ(x) function of the T1xd film is presented as an example.

The L_{pn} number average long period [37] of the lamellar structure of the TMXDI-SODI films was determined from the position of the first maximum of γ(x) functions. The E thickness of a transition layer between hard and soft domains was calculated from an x value, for which the value of the so-called autocorrelation triangle is equal to γ(0), in accordance with the relationship x=E/3 [39]. Neglecting the fact that all correlation functions shown in Fig. 8 do not exhibit a flat minimum (most probably due to the overlapping of the distance distributions of both hard and soft domains), the φ volume fraction of a minority phase of the lamellar stacks of the films investigated was calculated from the γ_m minimum of γ(x) functions, in accordance with the relationship $\gamma_m = -\varphi/(1-\varphi)$ [39]. It should be underlined that the so-called quadratic equation [40] could not be used to calculate the φ volume fraction for the investigated films, due to the 0.25 critical value of the A/L_p ratio (see Fig. 8). In accordance with the data given in Tab.3, the volume fraction of a minority phase of lamellar stacks of these films changes only insignificantly when the NCO / OH ratio increases from 1.5 / 1 to 3.5 / 1, and then drops when the ratio reaches the value of 4.5/1. Thus, it may be assumed that those φ values determine the volume fraction of siloxane-rich soft layers in lamellar stacks of siloxane-urethaneurea films. In other words, it may be postulated that the siloxane-rich soft phase is the minority phase in the lamellar stacks of these films. Hence, the mean values of the l_H thickness of TMXDI hard layers and the l_S thickness of siloxane rich soft layers were estimated following equations (3) and (4):

$$l_H = (1-\varphi)L_{pn} - E \qquad (3)$$

$$l_S = \varphi L_{pn} - E \qquad (4)$$

For clarity, the changes of the characteristics given in Tab. 3 are plotted in Fig. 9 as well. Only an insignificant in-

Table 3. *The characteristics of the lamellar structure of TMXDI-SODI siloxane-urethaneurea films investigated.*

Sample	NCO/OH	γ_m	φ	E/3	E	l_H	l_S	L_{pn}	L_{pw}
				[Å]	[Å]	[Å]	[Å]	[Å]	[Å]
T1xa	1.5/1	-0.649	0.394	3.8	11.4	14.4	5.3	42.6	46
T1xb	2.0/1	-0.695	0.410	3.8	11.4	19.5	10.1	52.5	54
T1xc	2.5/1	-0.694	0.410	4.3	12.9	22.0	11.3	59.1	61
T1xd	3.5/1	-0.685	0.407	4.3	12.9	23.6	12.1	61.5	64
T1de	4.5/1	-0.575	0.365	4.2	12.6	30.9	12.4	68.2	74

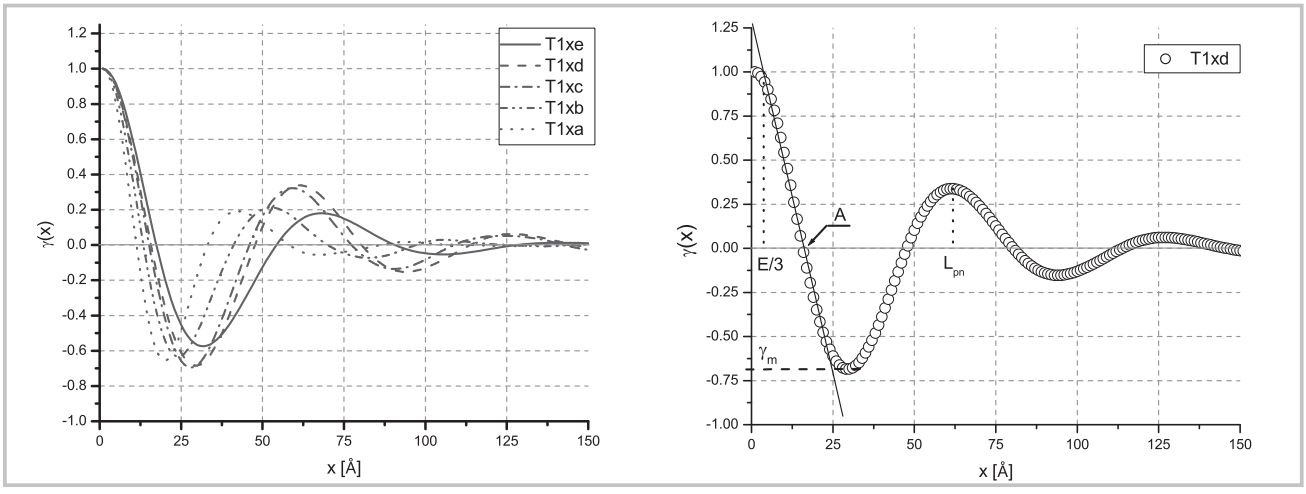

Figure 8. *The comparison of γ(x) correlation functions of TMXDI-SODI films investigated (left) and an example scheme of the correlation function analysis of the T1xd sample (right).*

crease of the transition layer thickness occurs when the NCO/OH ratio reaches the value of 2.5/1. Taking into account empirical errors, it may be assumed that the transition layer's thickness does not depend on the TMXDI unit concentration. The thickness of both TMXDI hard layers and siloxane rich soft layers increase with the increase in the NCO/OH ratio for smaller values of the NCO/OH ratio. When the NCO/OH ratio reaches the value of 3.5/1, the l_S thickness starts to become constant (ca. 13- [Å]), in contrast to the l_H thickness which then significantly increases. Moreover, it is interesting to note that the thickness of TMXDI hard layers and especially that of siloxane-rich soft layers in the lamellar stacks of the films investigated, are relatively thin in comparison to the thickness of transition layers between hard and soft domains. The L_{pn} number-averaged long period of the lamellar structure of the investigated films changes in the same way as the L_{pw} weight-averaged long period determined previously from scattering functions Iq^2 vs. q; in other words, a significant increase in the long period occurs for the smaller TMXDI unit concentration, then the rate of increase drops, and finally a significant increase in the long period is again observed (as should be expected [37], the values of L_{pn} are smaller then the values of L_{pw} , see Tab.3).

The results obtained from the analysis of γ(x) correlation functions of TMXDI-SODI films coincide well with the earlier discussed results of the WAXS investigations of these films, as well as the results of the molecular modelling of an extended (-TMXDI-UR-) chain, and also with the changes in the l_M length of siloxane-urethane prepolymers of the TMXDI-SODI films.

As mentioned earlier, a gradual increase in the Q_n invariant occurs when the TMXDI unit concentration increases. On the other hand, the l_M length of siloxane-urethane prepolymers gradually decreases with the increase in the NCO/OH ratio (Fig. 7). But it may be assumed that single TMXDI units which join two siloxane soft segments of siloxane-urethane prepolymers are mixed in the siloxane-rich soft phase. So, the longer the siloxane-urethane prepolymers, the more TMXDI units are mixed in the siloxane-rich soft phase; as a result of this, the electron density contrast between the TMXDI hard and the siloxane-rich soft phase increases when the NCO/OH ratio increases. Hence one may postulate that the coincidence shown on the right of Fig. 7 first of all reflects the changes of an electron density contrast between the TMXDI hard phase and the siloxane-rich soft phase of these siloxane-urethaneureas, although the values of the Q_n invariant depend on both the electron density contrast and the volume fractions of the phases.

It is obvious that the values of the l_H and the l_S thickness of TMXDI hard and siloxane-rich soft layers respectively, as determined from correlation functions, are averaged values. In accordance with the data given in Tab. 3, the mean thickness of hard layers in the T1xa film equals 14.4 [Å]. This value is a little less than the value of 14.7 [Å] for the l_{fp} fibre period of an extended (-TMXDI-UR-) chain shown in Fig. 6. Moreover, as shown in Fig. 9, the greater the NCO/OH ratio, the thicker the TMXDI hard layers (see the plot of the l_H vs. NCO/OH ratio). On the other hand, as may be deduced from the chemical structure of the siloxane-urethaneurea chain given in Fig. 1, the [-TMXDI-UR-TMXDI-] sequence is the shortest di-isocyanate sequence in that chain. The length of the next TMXDI sequence is the equivalent of the l_{fp} fibre period. As was pointed out, the smaller the NCO/OH ratio, the longer are the siloxane-urethane prepolymers which are synthesised. As a result of this, an excess of TMXDI units occurs even in the T1xa and the T1xb prepolymers (i.e. when the NCO/OH ratio equals 1.5/1 and 2.0/1 respectively). Therefore, TMXDI hard segments longer than the shortest di-isocyanate sequence occur not only in the T1xc, T1xd and T1xe siloxane-urethaneureas, but also in the T1xa and the T1xb siloxane-urethaneureas. However, it is clear that as the NCO/OH ratio gets smaller, the shorter TMXDI hard segments will predominate in the siloxane-ureaurethane chains. Consequently, as was found, the mean thickness of TMXDI hard layers is a little less than the l_{fp} fibre period for the NCO/OH ratio of 1.5/1, and for the NCO/OH ratio bigger than 1.5/1, the thickness of TMXDI hard layers is greater than the fibre period and gradually increases with the increase in the concentration of TMXDI units.

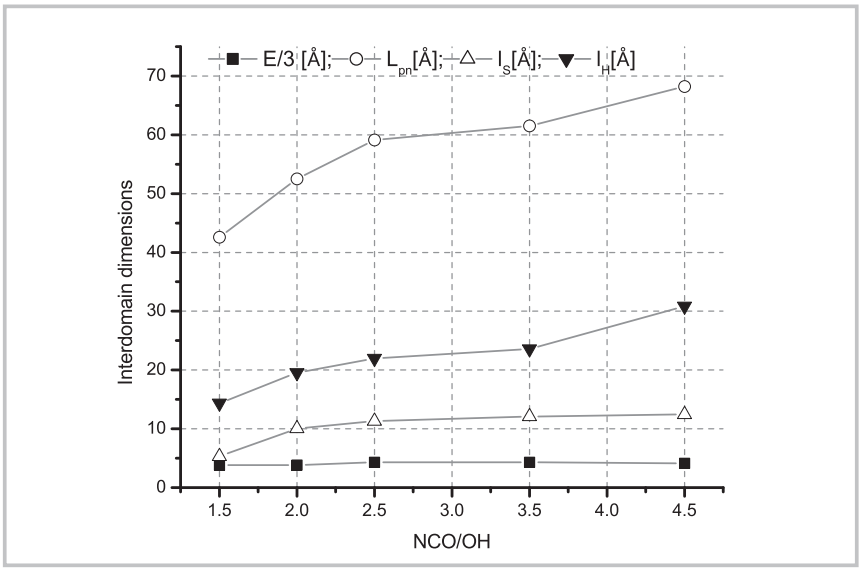

Figure. 9. *The plots of interdomain dimension changes of the lamellar structure of TMXDI-SODI films investigated.*

It is clear from the chemical structure of the TMXDI-SODI siloxane-urethaneurea chain (Fig. 1) that the transition layers in the lamellar stacks of the films investigated are formed by relatively long aliphatic-ether chains and urethane groups (urethane bonds act as linkages between TMXDI hard segments and siloxane soft segments). Moreover, one may suppose that both some short parts of siloxane segments and single TMXDI units are probably also mixed in transition layers and cause their thickening. Consequently, the transition layers between the TMXDI hard and the siloxane-rich soft layers are relatively thick, as compared with both the TMXDI hard and siloxane-rich soft layers, especially if the TMXDI unit concentration is small.

As pointed out earlier, an increase in the l_S thickness is observed for the smaller concentration of TMXDI units (Fig. 9), and then stabilisation of this thickness occurs. On the other hand, as a result of the WAXS investigations of TMXDI-SODI films, it was postulated that the increase in intensity of the diffraction peak centred at 19.7° (d = 4.51 [Å]) reflects

an increase of lateral dimensions of the TMXDI hard layers. Considering that siloxane chain is extremely flexible (as is well known, the energy barrier for the torsion angles of a siloxane backbone is close to zero in comparison to the energy barrier for the torsion angles of a methylene backbone), an extremely small thickness of siloxane rich soft layers may be expected. One may suppose that when the lateral dimensions of hard layers in lamellar stacks are relatively small, then some parts of randomly-folded siloxane soft segments will flow out from the stacks' sides. As the lateral dimensions of the hard layers in lamellar stacks increase, the longer parts of folded soft segments may fit the space between successive hard layers. When the lateral dimensions of hard layers become large enough, the thickness of soft layers should start to become constant. Finally, one may postulate that the behaviour of the l_s thickness of siloxane-rich soft layers (increase then saturation) is a consequence of an increase in the lateral dimensions of the TMXDI hard domains.

❑

Editorial note

To whom all correspondence should be addressed: R.Kwiatkowski (rkwiatkowski@ath.bielsko.pl)

Acknowledgement

Research was supported by the Polish State Committee for Scientific Research-Grant No. 7 T08 E070 18

References

1. C. Hepburn, Polyurethane Elastomers, Applied Science Publishers, London, (1982)
2. S. Abouzahr, G.L. Wilkes , "Segmented Copolymers with Emphasis on Segmented Polyurethanes", in Processing, Structure and Properties of Block Copolymers, M.J. Folkes Ed., Applied Science Publishers, London, (1985)
3. R. Bonart, L. Morbitzer, G. Hentze, J. Macromol. Sci. Phys., B9, 447, (1974)
4. R. Bonart, E.H. Müller, J. Macromol. Sci. Phys., B10, 177 (1974)
5. R. Bonart, E.H. Müller, J. Macromol. Sci. Phys., B10, 345 (1983)
6. J.T. Koberstein, R.S. Stein, J. Polym. Sci. Polym. Phys. Ed., 21, 1439 (1974)
7. L.M. Leung, J.T. Koberstein, J. Polym. Sci. Polym. Phys. Ed., 23, 1883 (1985)
8. L. Leibler, Macromolecules, 13, 1602, (1980)
9. G. Cho, A. Natanshon, T. Ho, K.J. Wynne, Macromolecules, 29, 2563, (1996)
10. J. Kozakiewicz, H. Janik, R. Kwiatkowski, A. Wlochowicz, Polym. Adv. Technol., 11, 82, (2000)
11. T.H. Ho, K.J. Wynne, Polym. Adv. Technol., 6(1), 25, (1985)
12. R. Beurashid, G.L. Nelson, J. Polym. Sci. Part A, Polym. Chem., 32, 1847, (1994)
13. A.Z. Okhema, D.J. Fabrizius, Biomaterials, 10, 23, (1989)
14. S.D. Park, I.K. Kang, K.H. Kim, Y.M. Lee, Y.K. Sung, Poliimo, 18, 868, (1994)
15. J.E. Mark, Adv. Chem. Ser., 224, 47, (1990)
16. E. Ranucci, P. Ferruti, C. Della Volpe, C. Migliaresi, Polymer, 35, 557, (1994)
17. N.M.K. Lamba, K.A. Woodhaus, S.L. Cooper, Polyurethanes in Biomedical Applications, CRS Press LLC, New York, (1998)
18. Y. Ch. Lai, J. Appl. Polym. Sci., 60, 1193, (1996)
19. J. Kozakiewicz, Prog. Org. Coatings, 27, 123, (1996)
20. J. Kozakiewicz, M. Cholinska, M. Skarzynski, S. Iwanska, Z. Czlonkowska-Kohutnicka, Proc. " Polyurethanes 94", 9-12 October, Boston, (MA), 101, (1994)
21. X. Yu, M.R. Nagarajan, C. Li, P.E. Gibson, S.L. Cooper, J. Polym. Sci., Polym. Phys. Ed., 24, 2681, (1986)
22. C. Li, X. Yu, T. Speckhard, S.L. Cooper, J. Polym. Sci., Polym. Phys. Ed., 26, 315, (1988)
23. G. Oertel, Polyurethane Handbook, Carl Hanser Verlag, New York, (1994)
24. L.H. Peebles, Jr., Macromolecules, 7, 872, (1974)
25. J.G. Dillon , Infrared Spectroscopic Atlas of Polyurethanes, Technomic Publishing Com., Inc.: Lancaster, (1989)
26. H. Stabinger, O. Kratky, Makromol. Chem., 179, 1655, (1978)
27. C.G. Vonk, J. Appl. Cryst., 6, 81, (1973)
28. M.A. Singh, S.W.S. Gosh, R.F. Shannon, J. Appl. Cryst., 26, 787 (1993)
29. C. Boulin, R. Kempf, M.H.J. Koch, S.M. Laughlin, Nucl. Instrum. and Methods, A249, 399, (1986)
30. R. W. Seymur, S.L. Cooper, Macromolecules, 6, 48, (1973)
31. J.W.C. Van Bogart, D.A. Bluemke, S.L. Cooper, Polymer, 22, 1428, (1981)
32. L.M. Leung, J.T. Koberstein, Macromolecules, 19, 706, (1986)
33. J.T. Koberstein, T.P.R Russell, Macromolecules, 19, 714, (1986)
34. J.T. Koberstein, A.F. Galambos, Macromolecules, 25, 5618, (1992)
35. T.K. Chen, T.S. Shien, J.Y. Chui, Macromolecules, 31, 1312, (1998)
36. A. Saiani, W.A. Daunch, H. Verbeke, J.W. Leenslag, J.S. Higgins, Macromolecules, 34, 9059, (2001)
37. C.G. Vonk, "Synthetic Polymers in Solid State", in Small Angle X-ray Scattering , O. Glatter, O. Kratky, Ed., Academic Press, London, (1983)
38. A. Guinier, G. Fournet, Small-Angle Scattering of X-rays, John Wiley & Sons, Inc., London, 1955
39. C.G. Vonk, A.P. Pijpers, J. Polym. Sci., Polym. Phys. Ed., 23, 2517, (1985)
40. B. Goderis, PhD thesis, Katholieke Universiteit Leuven, November (1999)

❑ ***Received 14.01.2003, Revieved 05.05.2003***